Babeş-Bolyai University Cluj-Napoca
Biomolecular Physics Department - BPD

Molecular structure monitoring by vibrational spectroscopy

I. Aplicaţii ale spectroscopiei vibraţionale în studiul moleculelor de interes farmaceutic

tiamina, papaverina, metoclopramida

II. Studiu Raman şi SERS asupra complecşilor metalici

- Scopul studiului

- -caracterizarea structurii moleculare prin modurile vibraţionale
- -atribuirea modurilor vibraţionale prin calcule teoretice
- -monitorizarea speciilor moleculare la diferite pH-uri
- -monitorizarea speciilor moleculare adsorbite la diferite pH-uri
- -geometria de adsorbţie pe suprafeţele metalice

Tiamina – vitamina B_1

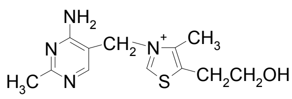

Spectrele Raman şi IR ale tiaminei in stare solidă

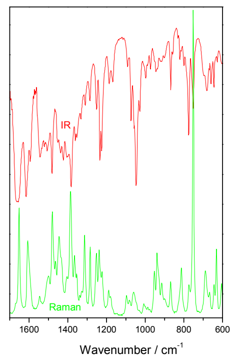

---

geometria optimizată

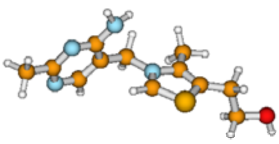

FT-Raman	FTIR	Calc.[a]	Calc.[b]	Assignment
327sh		327	327	δ_{op}(ring1)
344s		332	332	δ_{op}(ring2)
400w	411w	426	424	δ_{op}(ring1), δ_{op}(ring2)
518w	516w	527	527	δ_{ip}(ring1)
546s	540m	553	552	δ_{op}(NH)
606w	595w	605	604	δ_{op}(ring2), δ_{op}(CNC)ring1 bridging
632m	626w	622	621	δ_{op}(ring1), δ_{ip}(ring2)
644w	644m	647	648	δ_{op}(ring1)
667w	659m	657	658	δ_{ip}(ring2)
689m	681m	699	699	δ_{op}(ring2-C-C)
752s	752m	755	752	ν(ring1 breathing)
814m	800m	801	800	δ_{ip}(ring1), δ_{op}(ring2)
869w	868m		872	ν(C-S)
900sh	899sh	907	902	δ(CH_2-CH_2) bridging
915w	918w	915	912	δ_{op}(ring1-CH_3)
939m	934sh	940	932	ν(ring2 breathing)
1043sh	1047s	1056	1047	ν(C-O)
1083w	1073m	1091	1089	δ(NH_2)
1096w	1091m	1094	1090	δ(CH_2-CH_2, CH_3 ring1)
1177w	1168m	1146	1141	δ (ring2)+ν(CNC)+δ(CH_3)
1188w	1185m	1194	1193	ν(C-C)
1222m	1225s	1219	1218	δ(C-H)
1238m	1234s	1277	1271	ν(N-C-N)
1251m	1251m	1278	1278	δ(CH_2-CH_2+CH_3)
1284m	1284m	1286	1282	ν(C-C)
1353sh	1352m	1355	1350	δ(CH, CH_3 ring1, ring2)
1365m	1361m	1380	1370	ν(ring1)
1386s	1381s	1405	1398	ν(ring1)
1403sh	1405m	1406	1406	δ (CH, CH_2-CH_2, OH)
1431sh	1423m	1435	1427	ν(ring1)
1445m	1438m	1449	1441	δ(CH, CH_2)
1479s	1480s	1485	1479	ν(ring2)
1498m	1506m	1499	1491	δ (CH_2-CH_2)
1545w	1542m	1542	1538	ν(ring1)
1606m	1614s	1583	1596	ν(ring1)
1651s	1656s	1631	1637	ν(ring1), δ(NH_2)
2733w	2738m	2794	2762	ν(C-H)
2867sh	2853sh	2997	2984	ν(C-H)
2928s	2949s	3049	3003	ν(CH_2-CH_2)
2966s	2969s	3074	3037	ν(C-H) bridging
3080sh	3101s	3119	3103	ν(CH_3-ring2, -ring1)
	3442s	3496	3490	ν(N-H)
	3504s	3554	3540	ν(O-H)

Spectrele Raman ale tiaminei în soluţie apoasă la diferite pH-uri

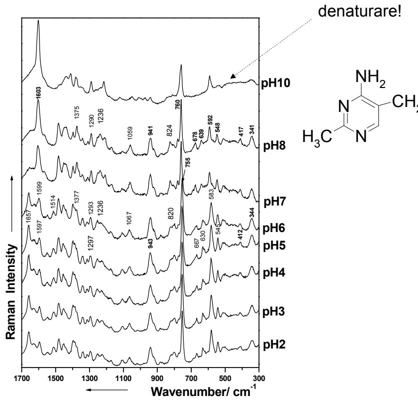

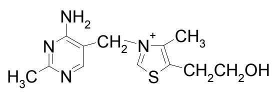

Spectre Raman ale tiaminei în soluţie apoasă la diferite pH-uri

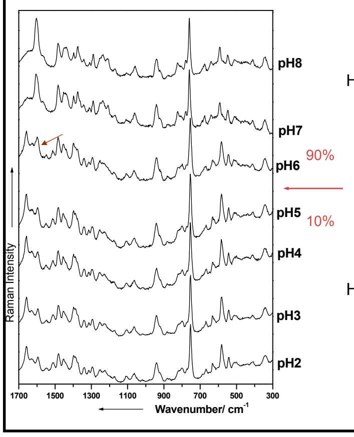

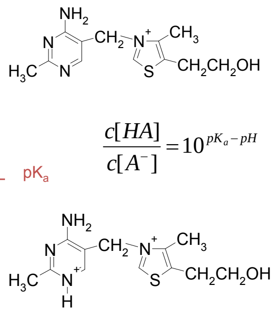

$$\frac{c[HA]}{c[A^-]} = 10^{pK_a - pH}$$

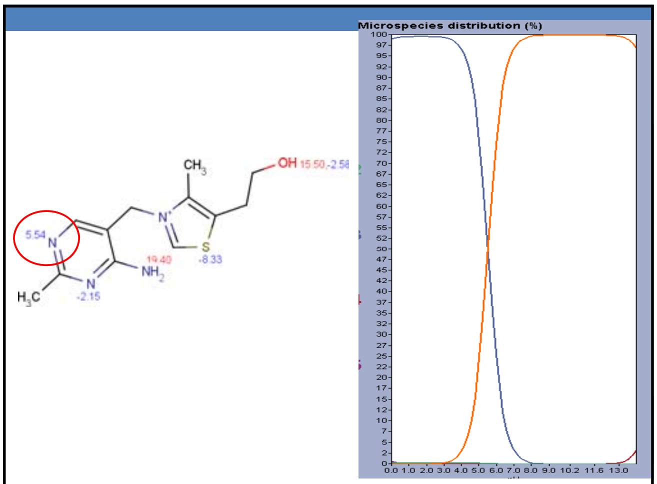

Spectrele SERS ale tiaminei în soluţie coloidală de aur la diferite pH-uri

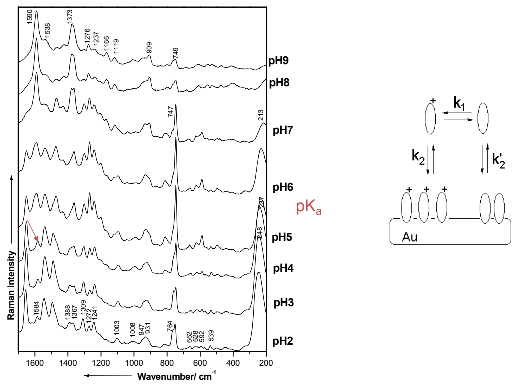

Geometria de adsorbţie a tiaminei pe suprafeţe nanometrice de Au

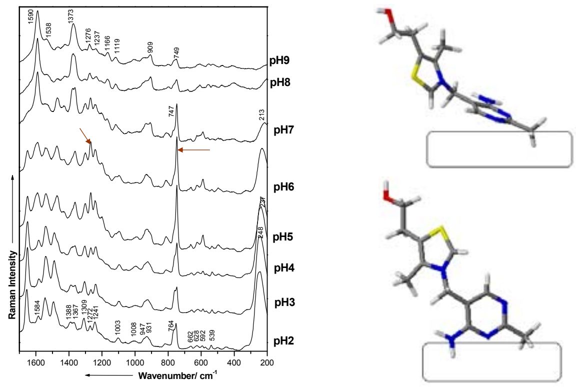

Papaverina

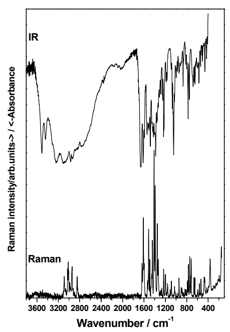

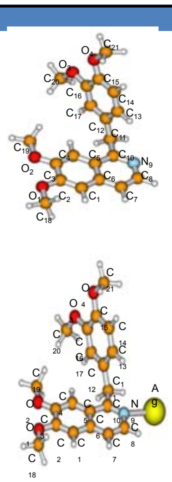

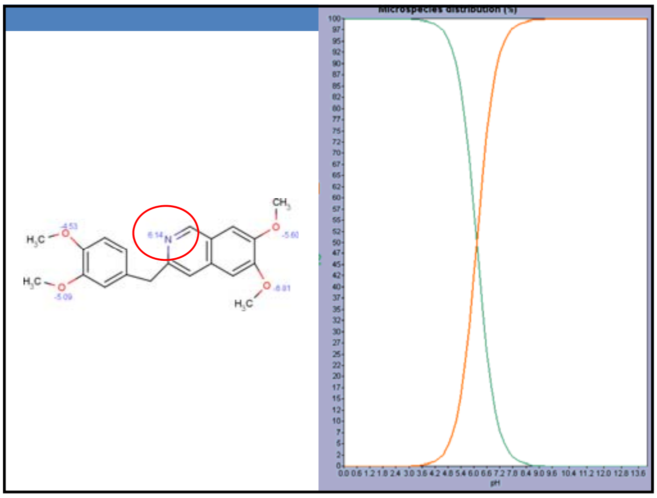

Spectrele Raman ale papaverinei
la diferite pH-uri

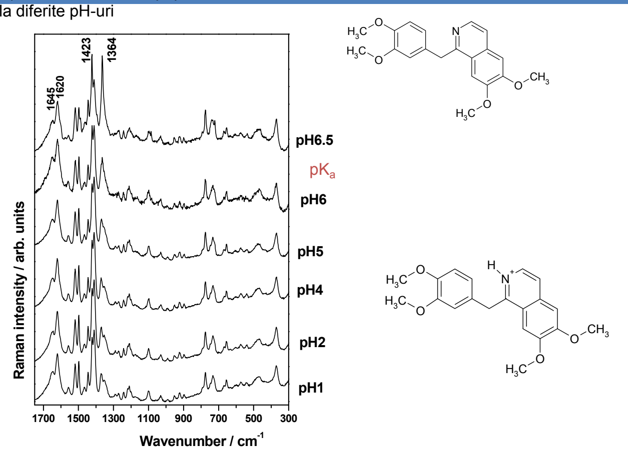

Spectrele SERS ale papaverinei
între pH 2 şi pH 10

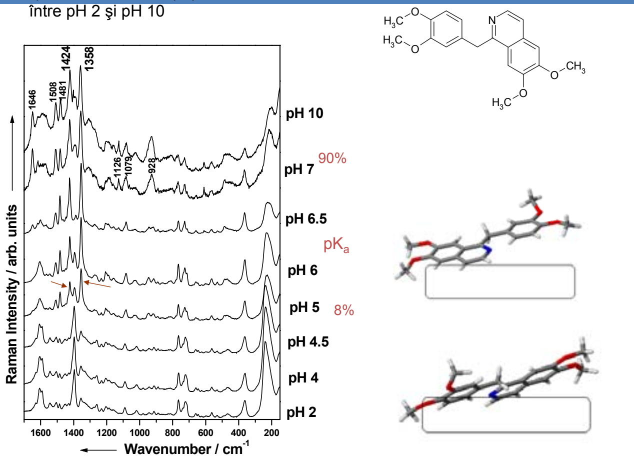

Metoclopramida

Raman

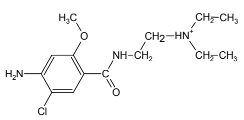

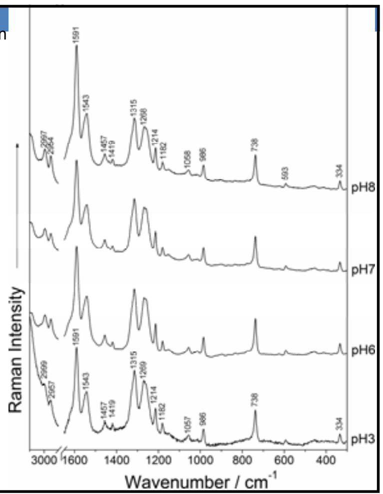

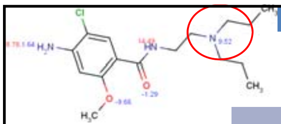

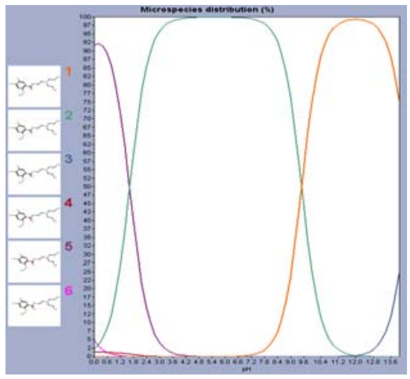

SERS

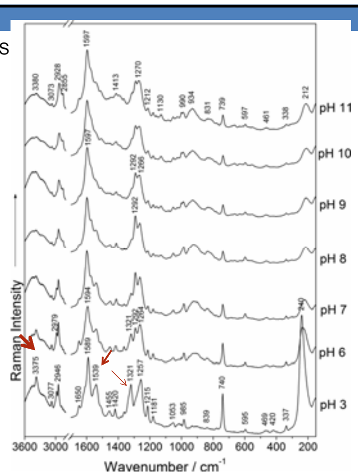

Concluzii

- ★ spectrele IR, Raman şi SERS în diferite condiţii experimentale –> informaţii structurale moleculare
- ★ atribuirea modurilor vibraţionale prin calcule teoretice
- ★ monitorizarea Raman a speciilor moleculare la diferite pH-uri
- ★ monitorizarea SERS a speciilor moleculare adsorbite la diferite pH-uri
- ★ geometria de adsorbţie pe suprafeţele metalice

IR, Raman and surface-enhanced Raman study of desferrioxamine B and its Fe(III) complex, ferrioxamine B

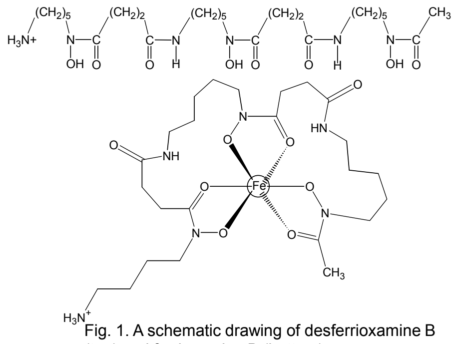

Fig. 1. A schematic drawing of desferrioxamine B (top) and ferrioxamine B (bottom).

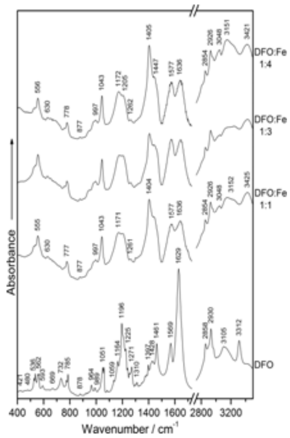

Fig. 2. FT-IR spectra of desferrioxamine B (DFO) and ferrioxamine B (DFO:Fe) with the stoichiometric ratios as indicated.

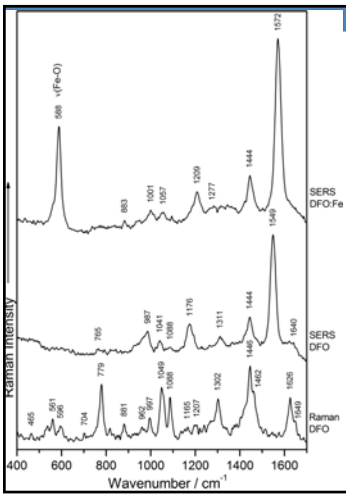

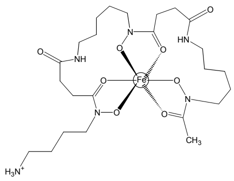

Fig. 3. FT-Raman and FT-SERS spectra of desferrioxamine B (DFO) and ferrioxamine B (DFO:Fe)

Raman spectroscopic and DFT theoretical study of 4-(2-pyridylazo)resorcinol and its complexes with zinc(II) and copper(II)

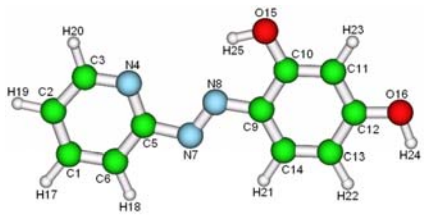

Fig.1. Chemical structure of PAR with atom numbering scheme.

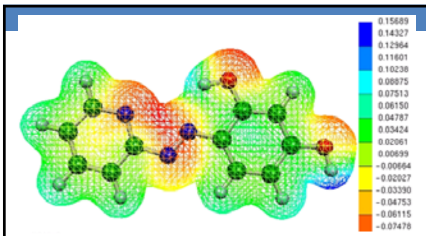

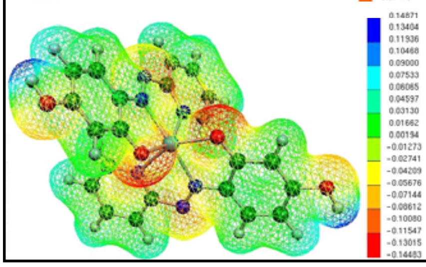

Fig.3. B3LYP/6-31G(d) calculated 3D molecular electrostatic potential of PAR (in a.u.).
Fig.4. B3LYP/6-31G(d) calculated 3D molecular electrostatic potential of $Zn(PAR)_2$ complex (in a.u.).

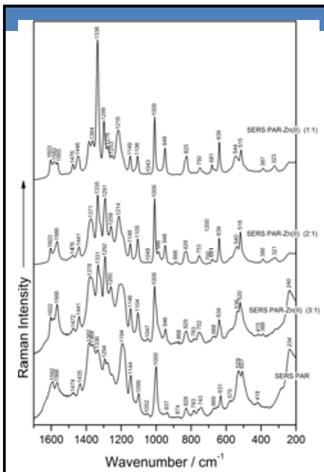

Fig.2. FT-Raman spectrum of PAR. SERS spectra of PAR and $Zn(PAR)_2$ complex, prepared at PAR:$ZnSO_4$ 3:1, 2:1 and 1:1 molar ratios.

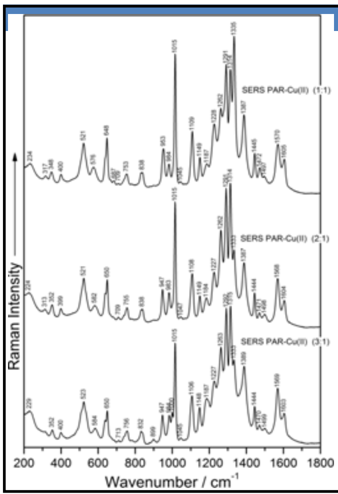

Fig.5. SERS spectra of the $Cu(PAR)_2$ complex, prepared at PAR:$CuSO_4$ 3:1, 2:1, 1:1 molar ratios.

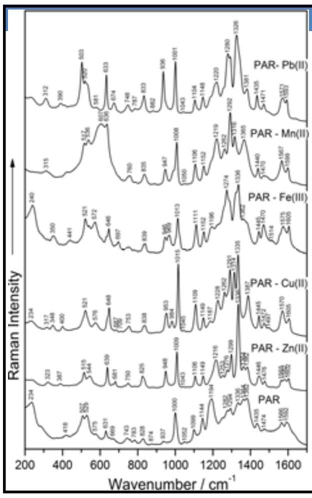

Fig.6. SERS spectra of Zn(II), Cu(II), Fe(III), Mn(II) and Pb(II) complexes of PAR, prepared at PAR:metal salt 1:1 molar ratio.

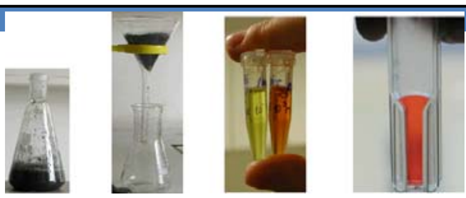

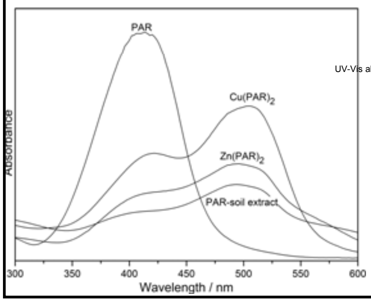

UV-Vis absorption spectra of PAR, $Zn(PAR)_2$, $Cu(PAR)_2$ and PAR-soil extract.

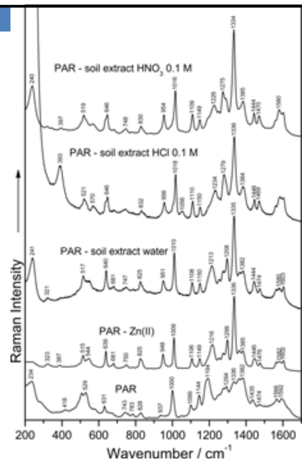

SERS spectra of the PAR-metal complexes obtained from different soil extracts. PAR and $Zn(PAR)_2$ SERS spectra were added as reference.

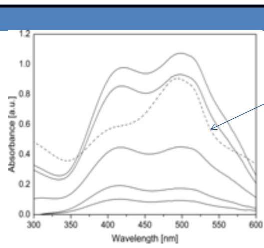

390 mg Zn(II) / kg soil

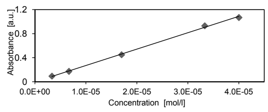

Conclusions

The FT-Raman and SERS spectra of PAR, as well as the SERS spectrum of $Zn(PAR)_2$ complex were safely assigned, due to a good match between experimental and DFT calculated vibrational modes. The SERS band assignment of the $Cu(PAR)_2$ complex was supposed to be similar to that of $Zn(PAR)_2$ complex, due to the similitude in band position between the two spectra.

The calculated MEP distributions indicate for the PAR molecule the highest electronegativity localized on the N and O atoms, whereas for the $Zn(PAR)_2$ complex the negative charge is localized mainly on the O atoms involved in the metal ion coordination, as expected from the deprotonated character of the oxygens.

The SERS spectra of the 3:1 molar ratios show mainly spectral features of the $Zn(PAR)_2$ or $Cu(PAR)_2$ complex, but also spectral features of PAR molecules adsorbed to the silver surface, whereas the SERS spectra of the 1:1 molar ratios show exclusively PAR-metal complex spectral features.

As several marker bands are characteristic to each PAR-metal complex, SERS could represent a prospective method for detection of metal ions, like Zn(II), Cu(II), Fe(III), Mn(II) and Pb(II).

SERS study on zidovudine

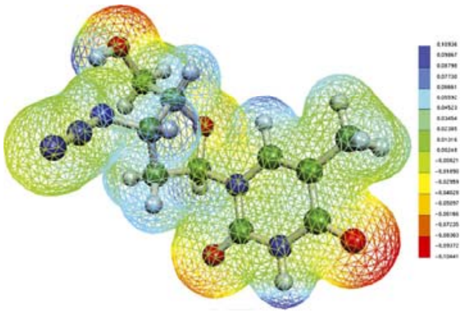

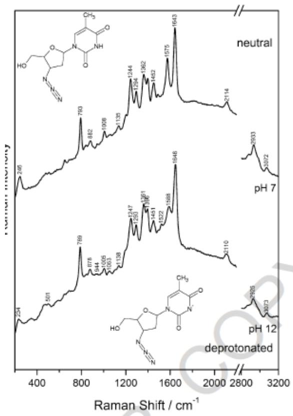

Vibrational spectroscopic study on melamine

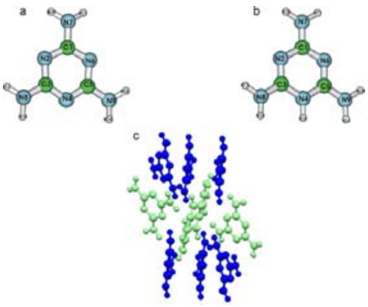

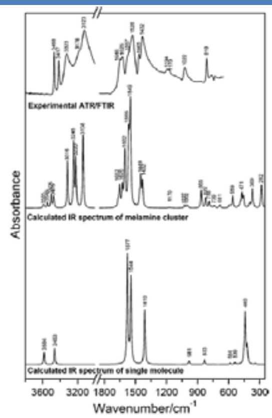

Fig. 2. ATR/FTIR spectrum of melamine powder (top), the calculated IR spectrum of a cluster of 10 melamine molecules (middle) and the calculated IR spectrum of a single molecule in neutral form (bottom).

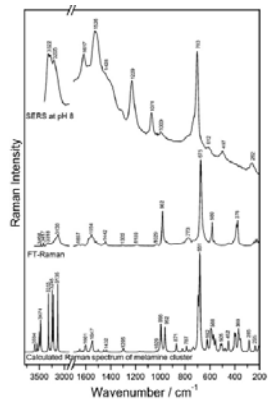

Fig. 3. Calculated Raman spectrum of 10 melamine molecules cluster (bottom), FT-Raman spectrum of melamine powder (middle) and SERS spectrum at pH 8 of neutral species of melamine (top).

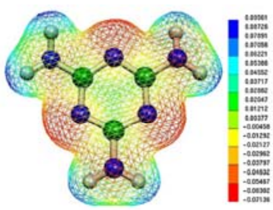

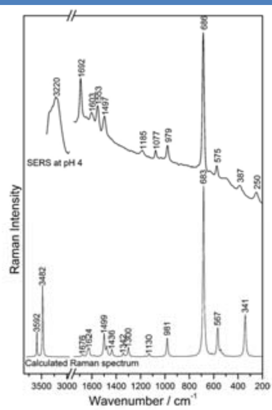

Fig. 4. SERS spectrum (top) at pH 4 and calculated Raman spectrum (bottom) of the protonated molecular form of melamine.

LABEL-FREE DETECTION OF BACTERIA BY USING IN SITU PREPARED SILVER NANOPARTICLES

PhD NICOLETA ELENA DINA (MIRCESCU)

UTI Pathogens Characterization: Challenges

- Is it possible to identify species independent of O-type antigen and strain (for *E. coli)?*
- Can most common uropathogens be identified?

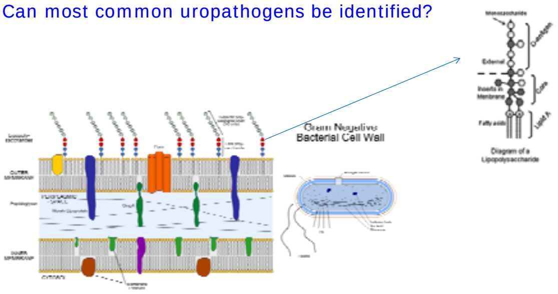

In situ 2-step-synthesis of Silver Nanoparticles

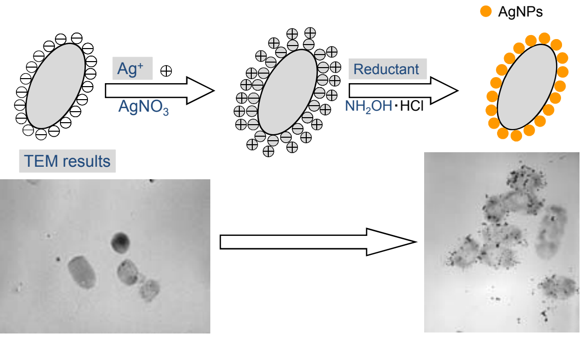

Z. Haibo, D. Yang, N. P. Ivleva, N.E. Mircescu, R. Niessner, C. Haisch, Anal Chem, 86 (3), 2014

SERS detection of UTI pathogens biomass

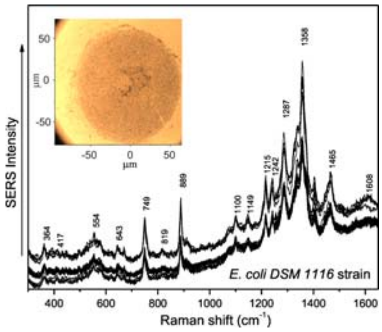

1) Adsorption of bacterial cells on the coated glass slide by electrostatic forces, no specific receptor required
2) 30 min interaction time
3) Wash the slide with Millipore water, then SERS spectra acquisition with high reproducibility

Total time: 2h 30 min

Conventional cultivation methods → more than 24 h!

Bacteria discrimination by PCA analysis based on the SERS spectra

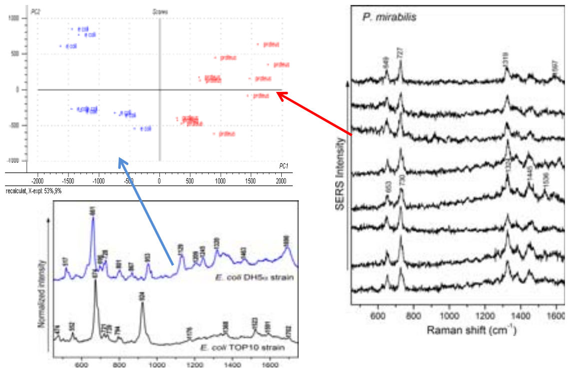

N. E. Mircescu, H. Zhou, N. Leopold, V. Chiş, N. P. Ivleva, R. Niessner, A. Wieser, C. Haisch, Anal Bioanal Chem, 406 (13), 2014;

Bacteria discrimination by PCA analysis based on the SERS spectra

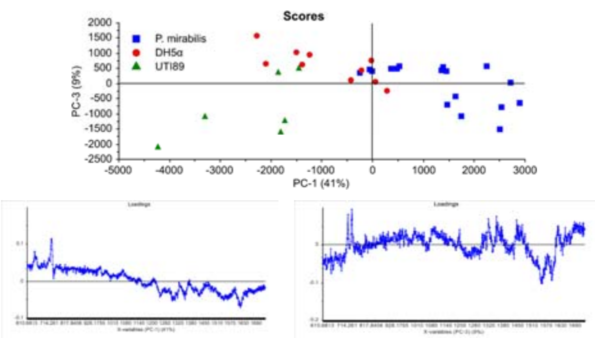

N. E. Mircescu, H. Zhou, N. Leopold, V. Chiş, N. P. Ivleva, R. Niessner, A. Wieser, C. Haisch, Anal Bioanal Chem, 406 (13), 2014;

Characterization Of Gram Positive Bacteria Using Raman Spectroscopy

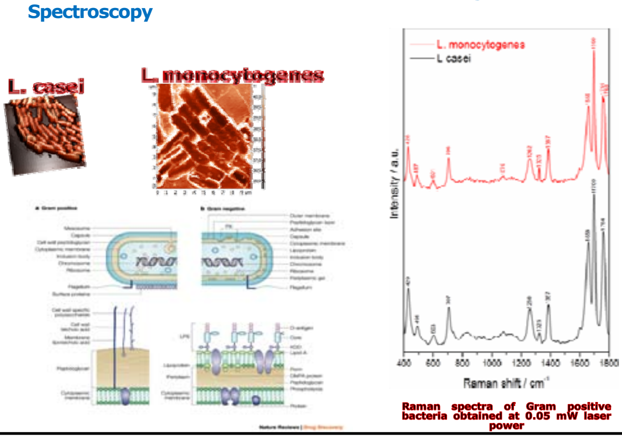

Raman spectra of Gram positive bacteria obtained at 0.05 mW laser power

Bacteria discrimination by PCA analysis based on the SERS spectra

SERS – In situ detection

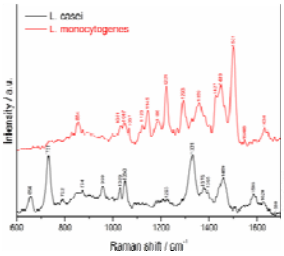

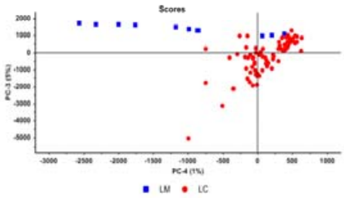

Two dimensional embeddings of samples by Category 1 PCA.

Characterization Of Halophilic Archaea Bacteria Using Raman Spectroscopy

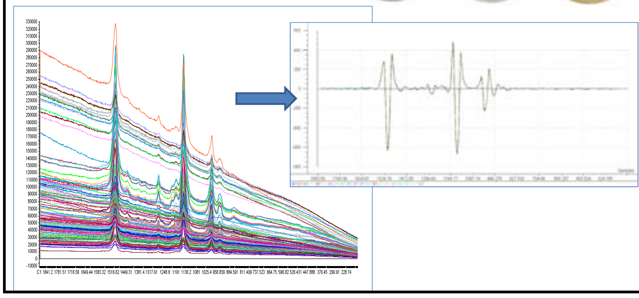

Analysis of the results

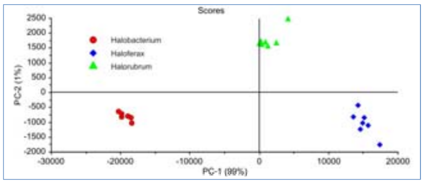

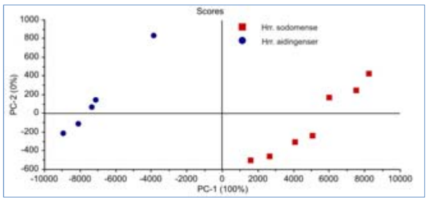

Analysis of the results

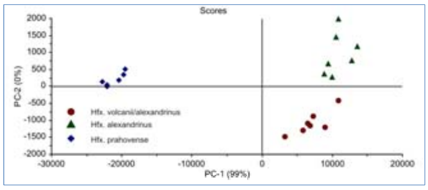

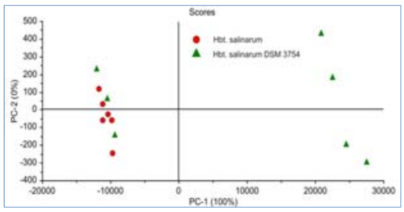

Conclusions

- Bacteria discrimination by PCA analysis based on the Raman/SERS spectra is possible independent of the species, O-antigen type, Gram-negative or Gram-positive type.
- A receptor-free SERS based detection method was tested on both Gram-negative and Gram-positive microorganisms for different biomedical purposes.
- The analysis time was significantly reduced by using the in situ SERS active silver nanoparticles.
- The PCA loadings show that the Raman/SERS marker bands are considered as main spectral features and compared in terms of intensity and Raman shifting for discrimination between different bacterial species/strains.

https://washington-seattle.digication.com/jonliu/Home

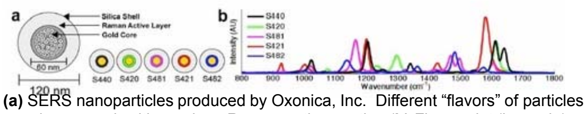

(a) SERS nanoparticles produced by Oxonica, Inc. Different “flavors” of particles are shown, each with a unique Raman-active coating (**b**) Fingerprint (barcode) Raman spectra from each of five different flavors of particles.

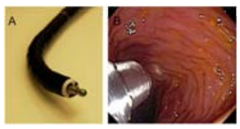

Spectral probe deployed through the instrument channel of an endoscope, and being used within the human colon https://washington-seattle.digication.com/jonliu/Home

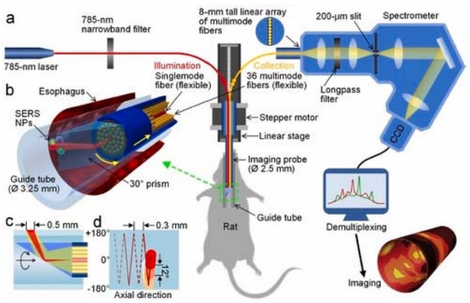

A spectral-detection system with a contact probe for quantifying the relative concentrations of multiplexed SERS NPs topicall applied on fresh intact tissues (*ex vivo* and *in vivo*). [Y Wang, et al., *Technology* 2, 1-15 (2014).]

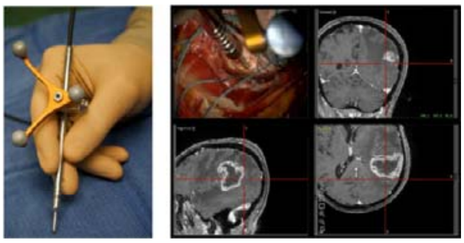

Raman spectroscopy handheld contact probe system for intraoperative detection. Picture of the probe used intraoperatively
J. Desroches, M. Jermyn, K. Mok, C. Lemieux-Leduc, J. Mercier, K. St-Arnaud, K. Urmey, M.C. Guiot, E. Marple, K. Petrecca, F. Leblond, *Characterization of a raman spectroscopy probe system for intraoperative brain tissue classification*, Biomedical Optics Express, 6 (2015).